Modeling a Lotka-Volterra Commensalism System with Prey Subject to Both Allee Effects and Linear Harvesting

Kan Fang, Xiaoying Chen*

Abstract—Dynamic behaviors of Lotka-Volterra commensal symbiosis model incorporating Allee effect and a linear harvesting in prey are studied in this paper. Through implementation of eigenvalue analysis alongside the Dulac-Bendixson criterion, the study establishes adequate criteria ensuring equilibrium exists and remains stable. Our results demonstrate that the interaction of Allee effects and harvesting triggers saddle-node bifurcations, progressively destabilizing the system. Crucially, we identify an extinction threshold for the prey population, prey extinction occurs. A key novel finding is a counterintuitive positive correlation: heightened Allee effects lead to increased prey population density — a rare and noteworthy ecological outcome. Computational simulations corroborate the primary conclusions.

Index Terms—Commensal Symbiosis Model; Allee Effect; Harvesting; Bifurcation.

I. Introduction

MONG key ecological models, commensalism holds significant prominence. During the last decades, many scholars investigater the dynamic behaviors of the commensalism model [1]–[10]. Han and Chen [10] proposed the continuous symbiotic modeling framework (1), proving that the distinctive positive equilibrium point for model (1) is globally asymptotically stable, while other boundary equilibrium points are unstable.

$$\dot{x} = x(b_1 - a_{11}x) + a_{12}xy,$$

$$\dot{y} = y(b_2 - a_{22}y).$$
(1)

The Allee effect [11] describes the phenomenon where the fitness of individuals decreases as the population density or size declines. In recent years, numerous scholars have been studying the changes in the dynamical behavior of biological mathematical models after incorporating the Allee effect [12]–[23]. Chen [23] investigated a new model (2) by adding the prey Allee effect to model (1), as follows:

$$\dot{x} = x(b_1 - a_{11}x) \frac{x}{x + C_0} + a_{12}xy,$$

$$\dot{y} = y(b_2 - a_{22}y).$$
(2)

Manuscript received April 30, 2025; revised August 11, 2025.

This study was funded by Science and Technology Program for Middleaged and Young Scholars of Fujian Provincial Department of Education Fujian Province (No.JAT220511), Natural Science Foundation of Fujian Province (No.2023J01163), and Science and Education Innovation Group Cultivation Project of Fuzhou University Zhicheng College (No.ZCKC23005).

Kan Fang is an associate professor of FuZhou University Zhicheng College, Fuzhou, Fujian 350002, China (e-mail: chrisfang517@sina.com).

Xiaoying Chen is an associate professor of the Department of Mathematics Research, Fujian Institute of Education, Fuzhou Fujian, 350001, China (corresponding author to provide: e-mail: snailkitty@126.com).

According to [23], the Allee effect has no bearing on the stability properties of the interior equilibrium point. Regulatory limits on fishing zones enable sustainable coexistence of human harvest and resource protection. Scholars have proposed models incorporating harvesting [24]–[29] druing the last decades.

However, prior studies have examined Allee effects and harvesting independently within ecological modeling frameworks, but their interactive impacts on commensal systems remain understudied. Based on the aforementioned research, this article primarily considers a new model (3) by adding a linear prey harvesting to model (2) and investigates the changes in its dynamical behavior. This work closes this gap via a systematic analysis of the interactions among these factors, resulting in emergent novel dynamics. A key finding is that harvesting induces two saddle-node bifurcations, a result scarcely documented for commensalism models. (Refer to Table I for the ecological implications associated with parameters in the equations and their units).

$$\dot{x} = x(b_1 - a_{11}x)\frac{x}{x + C_0} + a_{12}xy - r_0x,$$

$$\dot{y} = y(b_2 - a_{22}y).$$
(3)

TABLE I: Ecological meanings and units of parameters

Parameter	Ecological meaning	Units
\overline{x}	Prey concentration	indiv.·km ⁻²
y	Predator concentration	indiv.·km ⁻²
b_1	Prey's inherent growth rate	month ⁻¹
b_2	predator's inherent growth rate	month ⁻¹
a_{11}	Prey's self-competition parameter	km ² ·(indiv.·month) ⁻¹
a_{22}	predator's self-competition parameter	km ² ·(indiv.·month) ⁻¹
a_{12}	Commensalism benefit coeffi- cient for prey	km ² ·(indiv.·month) ⁻¹
C_0	Allee effect threshold density	indiv.·km ⁻²
r_0	Linear harvesting rate of prey	month ⁻¹

To simplify calculations, we perform transformation:

$$\begin{split} \bar{x} &= \bar{g}x, \quad \bar{y} = \bar{h}y, \quad \bar{t} = \bar{m}t, \quad \bar{m} = b_1, \\ a &= \frac{a_{12}b_2}{a_{22}b_1}, \quad \bar{g} = \frac{a_{11}}{b_1}, \quad \bar{h} = \frac{a_{22}}{b_2}, \quad b = \frac{b_2}{b_1}, \\ C &= \frac{a_{11}C_0}{b_1}, \quad r = \frac{r_0}{b_1}. \end{split}$$

Therefore we obtain an equivalent formulation of system (2), denoted as system (4) (identifying \bar{t} with t, \bar{x} with x, \bar{y} with

y.)
$$\dot{x} = \frac{x^2(1-x)}{x+C} + axy - rx,$$

$$\dot{y} = by(1-y).$$
 (4)

The remaining sections of this paper are arranged accordingly: Section 2 addresses solution boundedness. Section 3 covers equilibrium existence, qualitative analysis, and global stability of the positive equilibrium. Section 4 studies saddlenode bifurcation. Numerical illustrations and simulations in Section 5 demonstrate the theoretical outcomes. Lastly, Section 6 offers a summary and concluding discussions.

II. BOUNDEDNESS OF SOLUTIONS

To demonstrate the bounded nature of solutions to system (4), we first establish a fundamental lemma:

Lemma 2.1. [30] If
$$c^*$$
, $d^* > 0$, and $\frac{dx^*}{dt} \le x^*(t)(c^* - d^*x^*(t))$ with $x^*(t) > 0$, then $\limsup_{t \to +\infty} x^*(t) \le \frac{c^*}{d^*}$; If c^* , $d^* > 0$, and $\frac{dx^*}{dt} \ge x^*(t)(c^* - d^*x^*(t))$ with $x^*(t) > 0$, then $\liminf_{t \to +\infty} x^*(t) \ge \frac{c^*}{d^*}$.

Proposition 2.1. (1) Nonnegative invariance: Solutions (x(t), y(t)) with initial conditions $x(0), y(0) \ge 0$ satisfy $x(t) \ge 0$, $y(t) \ge 0$ for all $t \ge 0$.

(2) Bounded dynamics: All solutions with $x(0), y(0) \ge 0$ remain uniformly bounded in the positive quadrant for t > 0.

Proof: (1) Per ecological principles, initial conditions $x(0) \geq 0$, $y(0) \geq 0$ are imposed on (4) as population densities are nonnegative quantities. The dynamical equations in (4) can be expressed mathematically as:

$$\frac{\mathrm{d}x}{\mathrm{d}t} = x(\frac{x(1-x)}{x+C} + ay - r), \quad \frac{\mathrm{d}y}{\mathrm{d}t} = y(b(1-y)).$$

Performing integration over the interval [0, t] leads to:

$$\begin{split} &\int_0^t \frac{\mathrm{d}x}{x} = \int_0^t (\frac{x(1-x)}{x+C} + ay - r) \, \mathrm{d}t, \\ &\int_0^t \frac{\mathrm{d}y}{y} = \int_0^t (b(1-y)) \, \mathrm{d}t. \end{split}$$

After simplification, we obtain:

$$\ln \frac{x(t)}{x(0)} = \int_0^t (\frac{x(1-x)}{x+C} + ay - r) dt,$$
$$\ln \frac{y(t)}{y(0)} = \int_0^t (b(1-y)) dt.$$

By applying the exponential function to both sides, it follows that for all $t \ge 0$:

$$x(t) = x(0) \exp\left(\int_0^t \left(\frac{x(1-x)}{x+C} + ay - r\right) dt\right) \ge 0,$$

$$y(t) = y(0) \exp\left(\int_0^t b(1-y) dt\right) \ge 0.$$

Given the nonnegativity of initial conditions and the strictly positive nature of the exponential function, we deduce that Solutions (x(t),y(t)) with initial conditions $x(0),y(0)\geq 0$ satisfy $x(t)\geq 0$, $y(t)\geq 0$ for all $t\geq 0$, thereby proving statement (1).

(2) Applying Lemma 2.1 to the y-component of system (4) provides an asymptotic estimate: $\limsup_{t\to +\infty} y(t) \leq 1$. This

implies the existence of a finite upper bound L^* such that $y(t) \leq L^*$ for all $t \geq 0$. Analysis of (4)'s initial equation further establishes:

$$\dot{x} = \frac{x^2(1-x)}{C+x} + axy - rx \le x(1+aL^*-x).$$
 (5)

By reapplying Lemma 2.1, we derive the inequality $\limsup_{t\to +\infty} x(t) \leq 1+aL^*$. This ensures the existence of a finite constant Q^* such that $x(t) < Q^*$ holds for all t > 0.

Integrating these findings, we deduce that All solutions with $x(0), y(0) \ge 0$ remain uniformly bounded in the positive quadrant for t > 0.

III. EXISTENCE AND STABILITY OF EQUILIBRIA

A. Existence of equilibria

Equilibrium solutions within this domain are first examined. The following definitions are introduced:

$$p(x,y) = \frac{x^2(1-x)}{x+C} + axy - rx, \quad q(x,y) = by(1-y).$$

we obtain two boundary equilibrium points on the xx-axis: $A_0(0,0)$, $A_1(0,1)$. when y=0, we have $x^2-(1-r)x+rC=0$; when y=1, we have $x^2-(1-r+a)x+(r-a)C=0$. Defining

$$\triangle_1 = (1-r)^2 - 4rC, \ \triangle_2 = (1-r+a)^2 - 4(r-a)C,$$

$$x_2 = \frac{1-r}{2}, \ x_3 = \frac{1-r-\sqrt{\Delta_1}}{2}, \ x_4 = \frac{1-r+\sqrt{\Delta_1}}{2},$$

$$C_1 = \frac{(1-r)^2}{4r}, \ C_* = \frac{(1-r+a)^2}{4(r-a)}, \ x_3^* = \frac{1-r+a}{2},$$

$$x_1^* = \frac{1 - r + a + \sqrt{\triangle_2}}{2}, \ \ x_4^* = \frac{1 - r + a - \sqrt{\triangle_2}}{2},$$

leading to the following conclusion

Theorem 3.1.1.

- (1) The boundary equilibria $A_0(0,0)$ and $A_1(0,1)$ persist within the system (4) for all positive parameter settings.
- (2) When r < 1, $C = C_1$, system (4) admits a boundary equilibrium point $A_2(x_2,0)$; When q < 1, $C < C_1$, system (4) possesses boundary equilibrium points $A_3(x_3,0)$, $A_4(x_4,0)$.
- (3) When $r \geq a$, system (4) admits a single positive equilibrium $E_1(x_1^*,1)$; When $a < r < a+1,C > C_*$, system (4) possesses no positive equilibrium point; When $a < r < a+1,C = C_*$, system (4) possesses a single positive equilibrium $E_3(x_3^*,1)$; When $a < r < a+1,C < C_*$, system (4) exactly two positive equilibrium points $E_1(x_1^*,1)$, $E_4(x_4^*,1)$; When $r \geq a+1$, system (4) possesses no positive equilibrium point. A detailed local stability analysis for the equilibrium solutions of 4 is presented in the following subsection.

B. Local stability analysis of equilibria

Derivation of local stability criteria for boundary equilibria initiates our investigation.

Theorem 3.2.1.

- (1) $A_0(0,0)$ is a saddle.
- (2) If r < a, $A_1(0, 1 h_2)$ is a saddle; If r > a, $A_1(0, 1)$ is a stable node; If r = a, $A_1(0, 1)$ is a saddle-node.
- (3) If r < 1, $C = C_1$, $A_2(x_2, 0)$ is a saddle-node; If r < 1, $C < C_1$, $A_3(x_3, 0)$ is a unstable node, $A_4(x_4, 0)$ is a saddle.

Proof:

(1) At equilibrium point $A_0(0,0)$, the Jacobian associated with (4) is:

$$J(0,0) = \left[\begin{array}{cc} -r & & 0 \\ & & \\ 0 & & b \end{array} \right].$$

Analysis of the characteristic equation for J(0,0) identifies two real eigenvalues: $\lambda_1 = -r < 0$, $\lambda_2 = b > 0$ $(h_2 < 1)$, so $A_0(0,0)$ is a saddle.

(2) At equilibrium point $A_1(0,1)$, the Jacobian associated with (4) is::

$$J(0,1) = \left[\begin{array}{cc} a - r & 0 \\ 0 & -b \end{array} \right].$$

Analysis of the characteristic equation for J(0,1) identifies two real eigenvalues: $\lambda_1=a-r$, and $\lambda_2=-b<0$, if r< a, the boundary equilibrium $A_1(0,1)$ is a saddle; if r>a, $A_1(0,1)$ is a stable node; if r=a, $A_1(0,1)$ is non-hyperbolic. Stability determination employs the coordinate transformations u=x, v=y-1, $\mathrm{d}\tau=-b\mathrm{d}t$ (Assigning τ to t), translating the point $A_1(0,1)$ to $M_1(0,0)$. We expand system (4) as a Taylor series about the origin, retaining terms up to fourth order, resulting in the approximate system:

$$\begin{split} \dot{u} &= \overline{P}_2(u,v),\\ \dot{v} &= v + \overline{Q}_2(u,v). \end{split} \tag{6}$$

where

$$\overline{P}_{2}(u,v) = -\frac{a}{b}uv - \frac{u^{2}}{bC} + \frac{C+1}{bC^{2}}u^{3} - \frac{C+1}{bC^{3}}u^{4} + o(u^{4}),$$

$$\overline{Q}_{2}(u,v) = v + v^{2}.$$

The trivial solution $v=\Phi(u)=0$ is obtained from $\overline{Q}_2(u,v)=0$, leading to:

$$\overline{P}_2(u,v) = -\frac{u^2}{bC} + \frac{C+1}{bC^2}u^3 - \frac{C+1}{bC^3}u^4 + o(u^4).$$

Given a second-order lowest term with negative coefficient $-\frac{1}{bC}$, $B_1(0,0)$ is classified as a saddle-node equilibrium via Zhang's bifurcation theory (Theorem 7.1, Ch. 2 in [31]). We identify $B_1(0,0)$ as a saddle-node equilibrium. Thus $A_1(0,1)$ constitutes an attracting saddle-node with sector distribution: the attracting parabolic sector (via negative time mapping) fills the left half-plane, and the repelling hyperbolic sector populates the right half-plane.

(3) If r < 1, $C = C_1$, at equilibrium point $A_2(x_2, 0)$, the Jacobian associated with (4) is:

$$J(x_2,0) = \left[\begin{array}{cc} 0 & & \frac{a(1-r)}{2} \\ 0 & & b \end{array} \right],$$

When Jacobian analysis fails to determine stability for hyperbolic equilibrium $A_2(x_2,0)$, the coordinate transformation $\mathrm{d}\tau=\frac{1}{\beta+x},\mathrm{d}t$ (τ identified with t) is employed, resulting in the polynomial system:

$$\dot{x} = x^2(1-x) + axy(x+C) - rx(x+C),
\dot{y} = by(1-y)(x+C).$$
(8)

Given the topological equivalence between system (8) and (4), we execute successive transformations: $\bar{X} = x - \frac{1-r}{2}$, $\bar{Y} = y$ (Assigning \bar{X} to x, \bar{Y} to y), translating the point $A_2(x_2,0)$ to $M_2(0,0)$, then we do the coordinate transformation and time rescaling: u = 2bx - a(1-q)y, v = y, $d\tau = \frac{b(1-r+2C)}{2}b\,dt$ (Assigning τ to t). These operations convert system (8) to the polynomial form:

$$\dot{u} = \overline{P}_2'(u, v),$$

$$\dot{v} = v + \overline{Q}_2'(u, v).$$
(9)

where

$$\overline{P}_{2}'(u,v) = a_{20}u^{2} + a_{11}uv + a_{02}v^{2} + o(|u,v|^{2}),$$

$$\overline{Q}_{2}'(u,v) = b_{11}uv + b_{02}v^{2} + b_{12}uv^{2} + b_{03}v^{3}.$$

$$a_{20} = \frac{r-1}{2b^{2}(1-r+2C)}, \quad a_{11} = \frac{a(2bC-4rC-br+b)}{b^{2}(1-r+2C)},$$
(10)

$$a_{02} = \frac{a(1-r)(4b(a+b)C+(1-r)(2b(a+b)-ar-a))}{2b^2(1-r+2C)},$$

$$a_{02} = 2b^2(1-r+2C)$$

$$b_{11} = \frac{1}{b(1-r+2C)}, \quad b_{02} = -\frac{(a-b)(1-r)-2bC}{b(1-r+2C)},$$

$$b_{12} = -\frac{1}{b(1-r+2C)}, \quad b_{03} = -\frac{a(1-r)}{b(1-r+2C)}.$$

The trivial solution $v=\Phi(u)=0$ is obtained from $\overline{Q_2}'(u,v)=0,$ leading to:

$$\overline{P}_2'(u,v) = a_{20}u^2 + o(|u,v|^2)$$

Given a second-order lowest term with negative coefficient $\frac{r-1}{2b^2(1-r+2C)}$, $M_2(0,0)$ is classified as a saddle-node equilibrium via Zhang's bifurcation theory (Theorem 7.1, Ch. 2 in [31]). We identify $M_2(0,0)$ as a saddle-node equilibrium. Thus $A_2(x_2,0)$ constitutes an repelling saddle-node with sector distribution: the repelling parabolic sector (via positive time mapping) fills the left half-plane, and the hyperbolic sector populates the right half-plane.

If r < 1, $C < C_1$, at equilibrium point $A_3(x_3,0)$, the Jacobian associated with (4) is:

$$J(x_3,0) = \begin{bmatrix} r - \frac{x_3^2(C+1)}{(C+x_3)^2} & ax_3 \\ 0 & b \end{bmatrix},$$

Since

$$(1-r)^2 - (3r-1)C > 0,$$

$$((1-r)^2 - (3r-1)C)^2 - (1-r-C)^2 \triangle_1$$

$$= 4rC^2(C+1) > 0,$$

eigenvalues for $J(x_3,0)$ are computed as:

$$\begin{split} \lambda_1 &= r - \frac{x_3^2(C+1)}{(C+x_3)^2} \\ &= \frac{\sqrt{\Delta_1}((1-r)^2 - (3r-1)C - (1-r+C)\sqrt{\Delta_1})}{2(C+x_3)^2} > 0, \\ \lambda_2 &= b > 0, \end{split}$$

so the boundary equilibrium $A_3(x_3,0)$ is an unstable node.

At equilibrium point $A_4(x_4, 0)$, the Jacobian associated with (4) is:

$$J(x_4,0) = \begin{bmatrix} r - \frac{x_4^2(C+1)}{(C+x_4)^2} & ax_4 \\ 0 & b \end{bmatrix},$$

Consequently, the Jacobian at $(x_4, 0)$ yields two eigenvalues:

$$\lambda_1 = r - \frac{x_4^2(C+1)}{(C+x_4)^2}$$

$$= -\frac{\sqrt{\Delta_1}((1-r)^2 - (3r-1)C - (1-r+C)\sqrt{\Delta_1})}{2(C+x_4)^2} < 0,$$

so the boundary equilibrium $A_4(x_4,0)$ is a saddle.

Completing our stability investigation, we characterize local dynamics near interior equilibria $E_1(x_1^*,1)$, $E_3(x_3^*,1)$, $E_4(x_4^*,1)$.

Theorem 3.2.2.

 $\lambda_2 = b > 0$,

- (1) When $r \leq a$, the unique positive equilibrium point $E_1(x_1^*, 1)$ is locally asymptotically stable,
- (2) When $a < r < a+1, C = C_*$, the unique positive equilibrium point $E_3(x_3^*,1)$ is a saddle node; When $a < r < a+1, C < C_*$, the positive equilibrium point $E_1(x_1^*,1)$ is a saddle, while $E_4(x_4^*,1)$ is locally asymptotically stable.

Proof:

(1) When $r \leq a$, at equilibrium point $E_1(x_1^*, 1)$, the Jacobian associated with (4) is:

$$J(x_1^*, 1) = \begin{bmatrix} r - a - \frac{x_1^{*2}(C+1)}{(C+x_1^*)^2} & ax_1^* \\ 0 & -b \end{bmatrix},$$

when $r \leq a$, eigenvalues for $J(x_1^*,1)$ are computed as: $\lambda_1 = r - a - \frac{x_1^{*2}(C+1)}{(C+x_1^*)^2} < 0$, $\lambda_2 = -b < 0$, so the unique positive equilibrium point $E_1(x_1^*,1)$ is locally asymptotically stable.

(2) When $a < r < a + 1, C = C_*$, at equilibrium point $E_3(x_3^*, 1)$, the Jacobian associated with (4) is:

$$J(x_3^*, 1) = \begin{bmatrix} 0 & ax_3^* \\ & & \\ 0 & -b \end{bmatrix},$$

Given the topological equivalence between system (8) and (4), we execute successive transformations: $\bar{X} = x - \frac{1-r+a}{2}$, $\bar{Y} = y - 1$ (Assigning \bar{X} to x, \bar{Y} to y), translating the point $E_3(x_3^*,1)$ to $M_3^*(0,0)$, then we do the coordinate transformation and time rescaling: u = 2bx + a(1-r)y, v = y, $d\tau = -\frac{b(1-r+a+2C)}{2}$ dt (Assigning τ to t). Following these procedures, system (8) adopts the polynomial expression:

$$\begin{split} \dot{u} &= \overline{P}_2^{\ *}(u,v),\\ \dot{v} &= y + \overline{Q}_2^{\ *}(u,v). \end{split} \tag{11}$$

where

$$\overline{P}_{2}^{*}(u,v) = c_{20}u^{2} + c_{11}uv + c_{02}v^{2} + o(|u,v|^{2}),$$

$$\overline{Q}_{2}^{*}(u,v) = d_{11}uv + d_{02}v^{2} + d_{12}uv^{2} + d_{03}v^{3}.$$
(12)

$$c_{11} = \frac{a(b(r-1-a-2C)-(1-r+a)^2)}{b^2(1-r+a+2C)}, \quad c_{20} = \frac{1-r+a}{2b^2(1-r+a+2C)},$$

$$c_{02} = \frac{a(1-r+a)(4b(a+b)C+(1-r+a)(a+b)^2+a-ar)}{2b^2(1-r+a+2C)}$$

$$d_{11} = \frac{1}{b(1-r+a+2C)}, \quad d_{02} = \frac{2bC - (a-b)(1-r+a)}{b(1-r+a+2C)}$$

$$d_{03} = -\frac{a(1-r+a)}{b(1-r+a+2C)}, \quad d_{12} = \frac{1}{b(1-r+a+2C)}$$

The trivial solution $v=\Phi(u)=0$ is obtained from $\overline{Q}_2^{\ *}(u,v)=0,$ leading to:

$$\overline{P}_2^*(u,v) = c_{20}u^2 + o(|u,v|^2).$$

Given a second-order lowest term with positive coefficient $\frac{1-r+a}{2b^2(1-r+a+2C)}$, $B_3^*(0,0)$ is classified as a saddle-node equilibrium via Via Zhang's bifurcation theory (Theorem 7.1, Ch. 2 in [31]). We identify $B_3^*(0,0)$ as a saddle-node equilibrium. Thus $E_3(x_3^*,1)$ constitutes an attracting saddle-node with sector distribution: the attracting parabolic sector (via positive time mapping) fills the right half-plane, and the hyperbolic sector populates the left half-plane.

If $a < r < a+1, C < C_*$, at equilibrium point $E_4(x_4^*, 1)$, the Jacobian associated with (4) is:

$$J(x_4^*, 1) = \begin{bmatrix} r - a - \frac{x_4^{*2}(C+1)}{(C+x_4^*)^2} & ax_4^* \\ 0 & -b \end{bmatrix},$$

Since

$$(1-r+a)^2 - (3a-3r+1)C > 0,$$

$$((1-r+a)^2 + (3a-3r+1)C)^2 - (1-r+a+C)^2 \triangle_2$$

$$= 4(r-a)C^2(C+1) > 0,$$

consequently, the Jacobian at $(x_4^*, 1)$ yields eigenvalues:

$$= \frac{\sqrt{\Delta_2((1-r+a)^2 + (3(a-r)+1)C - (1-r+a+C)\sqrt{\Delta_2})}}{2(C+x_4^*)^2}$$

$$\lambda_2 = -b < 0.$$

 $\lambda_1 = r - a - \frac{x_4^{*2}(C+1)}{(C+x^*)^2}$

therefore the positive equilibrium $E_4(x_4^*, 1)$ is a saddle.

At equilibrium point $E_1(x_1^*, 1)$, the Jacobian associated with (4) is:

$$J(x_1^*, 1) = \begin{bmatrix} r - a - \frac{x_1^{*2}(C+1)}{(C+x_1^*)^2} & ax_1^* \\ 0 & -b \end{bmatrix},$$

consequently, the Jacobian at $(x_1^*, 1)$ yields eigenvalues:

$$\begin{split} \lambda_1 &= r - a - \frac{x_1^{*2}(C+1)}{(C+x_1^*)^2} \\ &= -\frac{\sqrt{\triangle_2}((1-r+a)^2 + (3(a-r)+1)C - (1-r+a+C)\sqrt{\triangle_2})}{2(C+x_4^*)^2} \\ &< 0, \end{split}$$

so the positive equilibrium $E_1(x_1^*, 1)$ is locally asymptotically stable.

C. Global stability analysis of equilibria

This section delineates a systematic investigation of global asymptotic stability for equilibrium states.

Theorem 3.3.1

 $\lambda_2 = -b < 0,$

(1) The single interior equilibrium $E_1(x_1^*, 1)$ of system (4) is globally asymptotically stable provided that

$$r \le a, \ b \ge \frac{1}{2}.\tag{13}$$

(2) The boundary equilibrium $A_1(0,1)$ is globally asymptotically stable provided that

$$r \ge a + 1, \ b \ge \frac{1}{2}, \ or$$

$$a < r < a + 1, \ C > C_*, \ b \ge \frac{1}{2}.$$
(14)

Proof: Under condition (14), local stability of $A_1(0,1)$ follows from Theorem 3.2.1. When (13) is satisfied, Theorem 3.2.2 guarantees existence and local stability of $E_1(x_1^*,1)$. Application of Dulac function $u(x,y)=\frac{1}{x^2y}$ yields:

$$\begin{split} D(x,y) &= \frac{\partial (u(x,y)\bar{p}(x,y))}{\partial x} + \frac{\partial (u(x,y)\bar{q}(x,y))}{\partial y} \\ &= -\frac{x^3 + (2C+b)x^2 + C(2b-1)x + bC^2}{xy^2(B+x)^2} \\ &< 0 \ (b \geq \frac{1}{2}) \end{split}$$

The Dulac-Bendixson theorem [32] excludes closed orbits in the positive quadrant. Given Theorem 3.1.1's boundedness guarantee, we deduce:(1) $E_1(x_1^*,1)$ is globally asymptotically stable if (13) is satisfied; (2) $A_1(0,1)$ achieves global asymptotic stability when (14) holds.

IV. SADDLE-NODE BIFURCATION

This section analyzes bifurcation behavior at equilibria of system (4).

Theorem 4.1.1

- (1) A saddle-node bifurcation is observed near boundary equilibrium $A_2(x_2,0)$ of system (4) at critical parameter $C_{SN}=C_1$, with B functioning as the control parameter.
- (2) A saddle-node bifurcation is observed near interior equilibrium $E_3(x_3^*,1)$ of system (4) at critical parameter $C=C_{SN^*}=C_*$, with B functioning as the control parameter.

Proof:

(1) When R < 1, $C = C_1$, at equilibrium point $A_2(x_2, 0)$, the Jacobian associated with (4) is:

$$J(A_2, B_{SN}) = \left[\begin{array}{cc} 0 & ax_2 \\ & & \\ 0 & b \end{array} \right],$$

The Jacobian matrices $J(A_2,B_{SN})$ and $J(A_2,B_{SN})^T$ each exhibit a single zero eigenvalue per linear algebraic analysis. Let V and W denote the corresponding eigenvectors for $J(A_2,B_{SN})$ and $J(A_2,B_{SN})^T$ respectively, direct computation yields

$$V = \left(\begin{array}{c} V_1 \\ V_2 \end{array}\right) = \left(\begin{array}{c} 1 \\ 0 \end{array}\right)$$

and

$$W = \left(\begin{array}{c} W_1 \\ W_2 \end{array} \right) = \left(\begin{array}{c} 1 \\ \frac{a(r-1)}{2h} \end{array} \right).$$

Furthermore, we have

$$F_C(A_2, C_{SN}) = \begin{pmatrix} \frac{x_2^2(x_2 - 1)}{(x_2 + C_1)^2} \\ 0 \end{pmatrix},$$

and

$$D^2F_C(A_2, C_{SN})(V, V)$$

$$= \left(\begin{array}{c} \frac{\partial^2 F_1}{\partial x^2} V_1^2 + 2 \frac{\partial^2 F_1}{\partial x \partial u} V_1 V_2 + \frac{\partial^2 F_1}{\partial u^2} V_2^2 \\ \\ \frac{\partial^2 F_2}{\partial x^2} V_1^2 + 2 \frac{\partial^2 F_2}{\partial x \partial u} V_1 V_2 + \frac{\partial^2 F_2}{\partial u^2} V_2^2 \end{array}\right)_{(A_2, C_{SN})}$$

$$= \left(\begin{array}{c} -\frac{2C_1(C_1+1)x_2}{(x_2+C_1)^3} \\ 0 \end{array}\right).$$

Obviously, we can get that

$$W^{T}D^{2}F_{C}(A_{2}, C_{SN})(V, V) = -\frac{2C_{1}(C_{1} + 1)x_{2}}{(x_{2} + C_{1})^{3}} \neq 0,$$

$$W^{T}F_{C}(A_{2}, C_{SN})(V, V) = \frac{x_{2}^{2}(x_{2} - 1)}{(x_{2} + C_{1})^{2}} \neq 0$$

Near the boundary equilibrium $A_2(x_2,0)$, system (4) experiences a saddle-node bifurcation, as confirmed by Sotomayor's theorem [33].

(2) When a < r < a + 1, $C = C_*$, at equilibrium point $E_3(x_3^*, 1)$, the Jacobian associated with (4) is:

$$J(E_3, C_{SN}^*) = \begin{bmatrix} 0 & ax_3^* \\ & & \\ 0 & -b \end{bmatrix},$$

It follows from linear algebra that a zero eigenvalue exists in both $J(E_3, C_{SN}^*)$ and $J(E_3, C_{SN}^*)^T$. When V and W are

defined as the corresponding eigenvectors for each matrix, computational results demonstrate

$$V = \left(\begin{array}{c} V_1 \\ V_2 \end{array} \right) = \left(\begin{array}{c} 1 \\ 0 \end{array} \right)$$

and

$$W = \left(\begin{array}{c} W_1 \\ W_2 \end{array}\right) = \left(\begin{array}{c} 1 \\ \frac{a(1-r+a)}{2h} \end{array}\right).$$

Furthermore, we have

$$F_C(E_3, C_{SN}^*) = \begin{pmatrix} \frac{x_3^{*2}(x_3^* - 1)}{(x_3^* + C_*)^2} \\ 0 \end{pmatrix}.$$

and

$$D^2F_C(E_3, C_{SN}^*)(V, V)$$

$$= \left(\begin{array}{c} \frac{\partial^2 F_1}{\partial x^2} V_1^2 + 2 \frac{\partial^2 F_1}{\partial x \partial u} V_1 V_2 + \frac{\partial^2 F_1}{\partial u^2} V_2^2 \\ \\ \frac{\partial^2 F_2}{\partial x^2} V_1^2 + 2 \frac{\partial^2 F_2}{\partial x \partial u} V_1 V_2 + \frac{\partial^2 F_2}{\partial u^2} V_2^2 \end{array}\right)_{(E_3, C_{SN})}$$

$$= \left(\begin{array}{c} -\frac{2C_*(C_*+1)x_3^*}{(x_3^*+C_*)^3} \\ 0 \end{array}\right).$$

Obviously, we can get that

$$W^T D^2 F_C(A_3^*, C_{SN}^*)(V, V) = -\frac{2C_*(C_* + 1)x_3^*}{(x_3^* + C_*)^3} \neq 0,$$

$$W^{T}F_{C}(A_{3}^{*}, C_{SN}^{*})(V, V) = \frac{x_{3}^{*2}(x_{3}^{*} - 1)}{(x_{3}^{*} + C_{*})^{2}} \neq 0$$

Near the boundary equilibrium $E_3(x_3^*, 1)$, system (4) experiences a saddle-node bifurcation, as confirmed by Sotomayor's theorem [33].

V. NUMERICAL SIMULATIONS

We verify analytical results through numerical experiments below.

We begin by analyzing the system (16) (a particular instance of system (4) characterized by $a=1,b=1>\frac{1}{2},r=3\geq a+1$ and C=0.125 separately.

Example 5.1

$$\dot{x} = \frac{x^2(1-x)}{x+0.125} + xy - 3x,$$

$$\dot{y} = 2y(1-y).$$
(16)

As shown in Figure 1 that trivial equilibrium $A_0(0,0)$ of system (16) is a saddle, and boundary equilibrium $A_1(0,0.5)$ is globally asymptotically stable, which drives the prey population to extinction.

Secondly we analyze the system (17) (a particular instance of system (4)) characterized by $a=1,b=1>\frac{1}{2},a< r=1.5< a+1$ separately.

Example 5.1.2

$$\dot{x} = \frac{x^2(1-x)}{x+C} + xy - 1.5x,$$

$$\dot{y} = y(1-y).$$
(17)

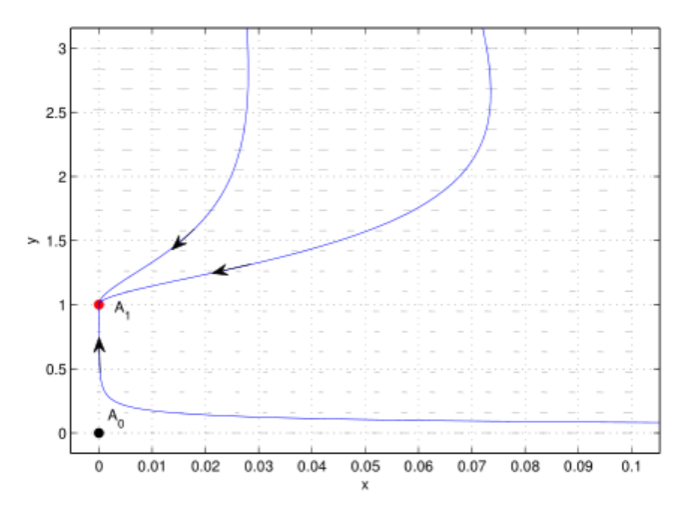


Fig. 1: Case **1** of $r \ge a + 1$.

 $A_0(0,0)$ of system (17) is a saddle, and $A_1(0,0.5)$ is a stable node (see Figure 2). (a) if $C=0.1<0.125=C_*$, as shown in Figure 2a, the interior equilibrium $E_4(0.138,1)$ is a saddle, $E_1(0.36,1)$ is a stable node. (b) if $C=0.125=C_*$, as shown in Figure 2b, $E_3(0.25,1)$ is a saddle. (c) if $C=0.5>C_*$, there is no interior equilibrium, whose phase diagram is similar to Figure 1. System bifurcates saddle-node at E_3 when $C=C_*=0.125$.

Thirdly we analyze the system (18) (a particular instance of system (4)) characterized by $a=0.2, b=1>\frac{1}{2}, a< r=0.5<1< a+1$ separately.

Example 5.1.3

$$\dot{x} = \frac{x^2(1-x)}{x+C} + 0.2xy - 0.5x,$$

$$\dot{y} = y(1-y).$$
(18)

For system (18), $A_0(0,0)$ is a saddle, and $A_1(0,0.5)$ is a stable node (see Figure 3). (a) if $C = 0.05 < C_1 <$ C_* , as shown in Figure 3a, $A_3(0.056,0)$ is an unstable node, $A_4(0.44,0)$ is a saddle. The interior equilibrium $E_4(0.022,1)$ is a saddle, $E_1(0.678,1)$ is a stable node. (b) if $C = 0.125 = C_1 < C_*$, as shown in Figure 3b, the equilibrium $A_2(0.25,0)$ is characterized as a saddle-node: repelling parabolic dynamics dominate the left half-plane, while hyperbolic repulsion governs the right half-plane. The interior equilibrium $E_4(0.058,1)$ is a saddle, $E_1(0.64,1)$ is a stable node. (c) if $C_1 < C = 0.2 < C_*$, as shown in Figure 3c, the interior equilibrium $E_4(0.1, 1)$ is a saddle, $E_1(0.6, 1)$ is a stable node. (d) if $C = 0.5 > C_*$, there is no interior equilibrium, the phase diagram is similar to Figure 1. System experiences saddle-node bifurcation at A_2 for the bifurcation parameter value $C = 0.125 = C_1$.

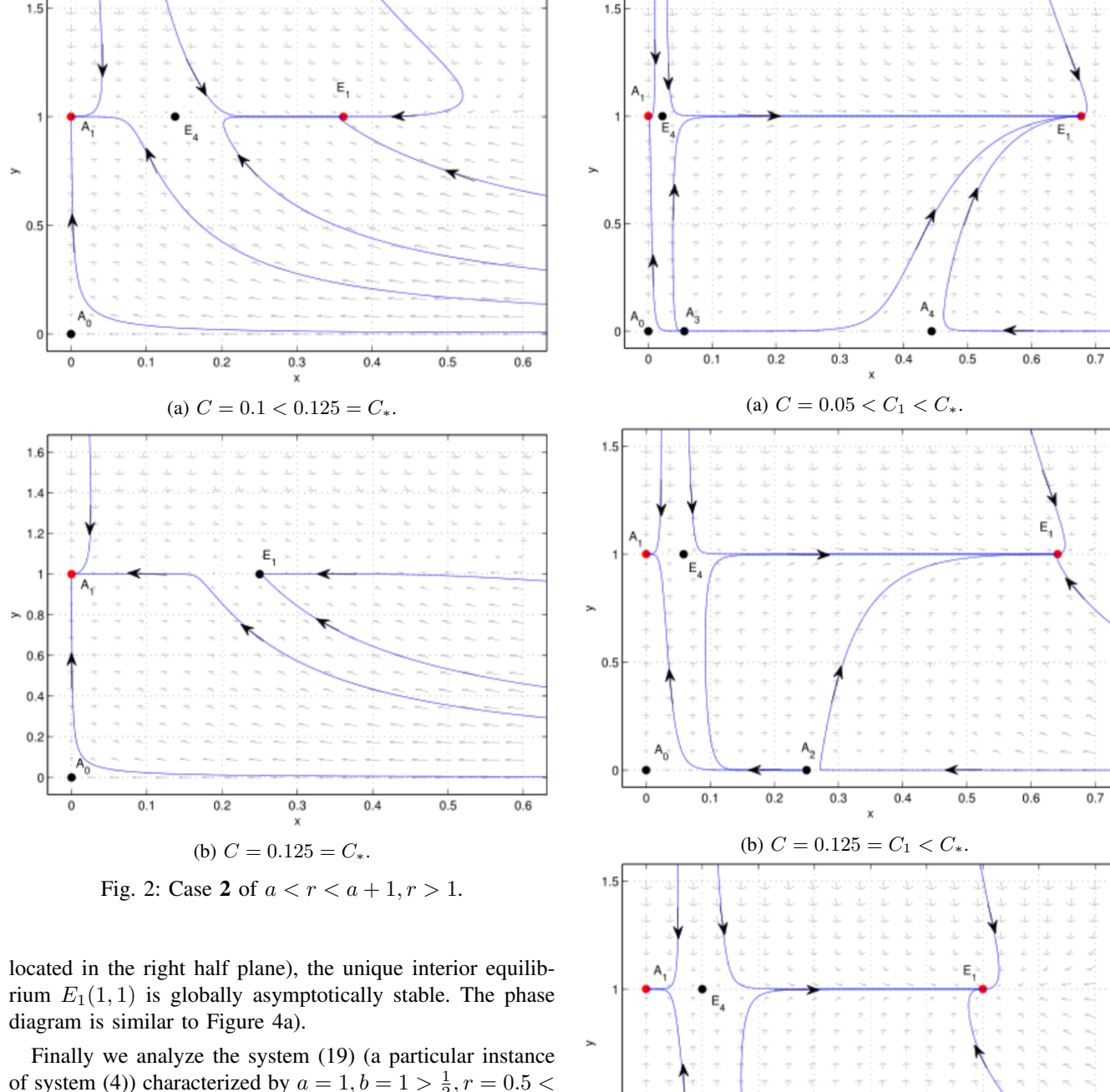
Fourthly we analyze the system (19) (a particular instance of system (4)) characterized by $a=1,b=1>\frac{1}{2},r=a=1,C=0.125$ separately.

Example 5.1.4

$$\dot{x} = \frac{x^2(1-x)}{x+0.125} + xy - x,$$

$$\dot{y} = y(1-y).$$
(19)

 $A_0(0,0)$ of system (19) is a saddle, while boundary equilibrium $A_1(0,0.5)$ is a saddle-node (whose hyperbolic sector



of system (4)) characterized by $a = 1, b = 1 > \frac{1}{2}, r = 0.5 <$ a, r < 1 separately.

Example 5.1.5

$$\dot{x} = \frac{x^2(1-x)}{x+C} + xy - 0.5x,$$

$$\dot{y} = y(1-y).$$
(20)

Trivial equilibrium $A_0(0,0)$ of system (18) is a saddle, and boundary equilibrium $A_1(0,0.5)$ is a saddle (see Figure 4). (a) if $C = 1.5 > C_1$, as shown in Figure 4a, the single interior equilibrium $E_1(1.896,1)$ is globally asymptotically stable. (b) if $C = 0.125 = C_1$, as shown in Figure 4b, $A_2(0.25,0)$ is a saddle-node (with its repelling parabolic (hyperbolic) sector governs the left(right) half plane). The unique interior equilibrium $E_1(1.54,1)$ is globally asymptotically stable. (c) if $C = 0.1 < C_1$, as shown in Figure 4c, $A_3(0.138,0)$ is an unstable node, $A_4(0.36,0)$ is a saddle. The unique interior equilibrium $E_1(1.54, 1)$ is globally asymptotically stable. The critical parameter value $C = 0.125 = C_1$ triggers saddle-node bifurcation at A_2 .

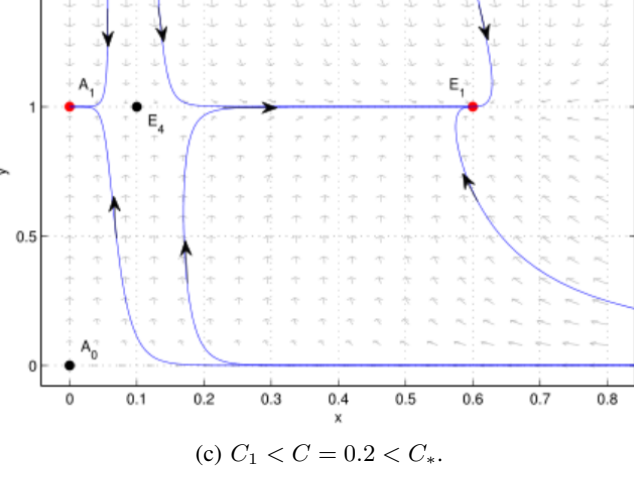


Fig. 3: Case **2** of a < r < 1 < a + 1.

VI. CONCLUSION

The introduction of the Allee effect and non-selective harvesting into a commensalism model in prey significantly complicates its dynamical behavior. System (4) demonstrates notable variations in the numerical configuration of equilibria (boundary/internal) induced by key parameter modulation.. Specifically, the system can undergos two saddle-node bifurcations depending on parameter values. A key finding

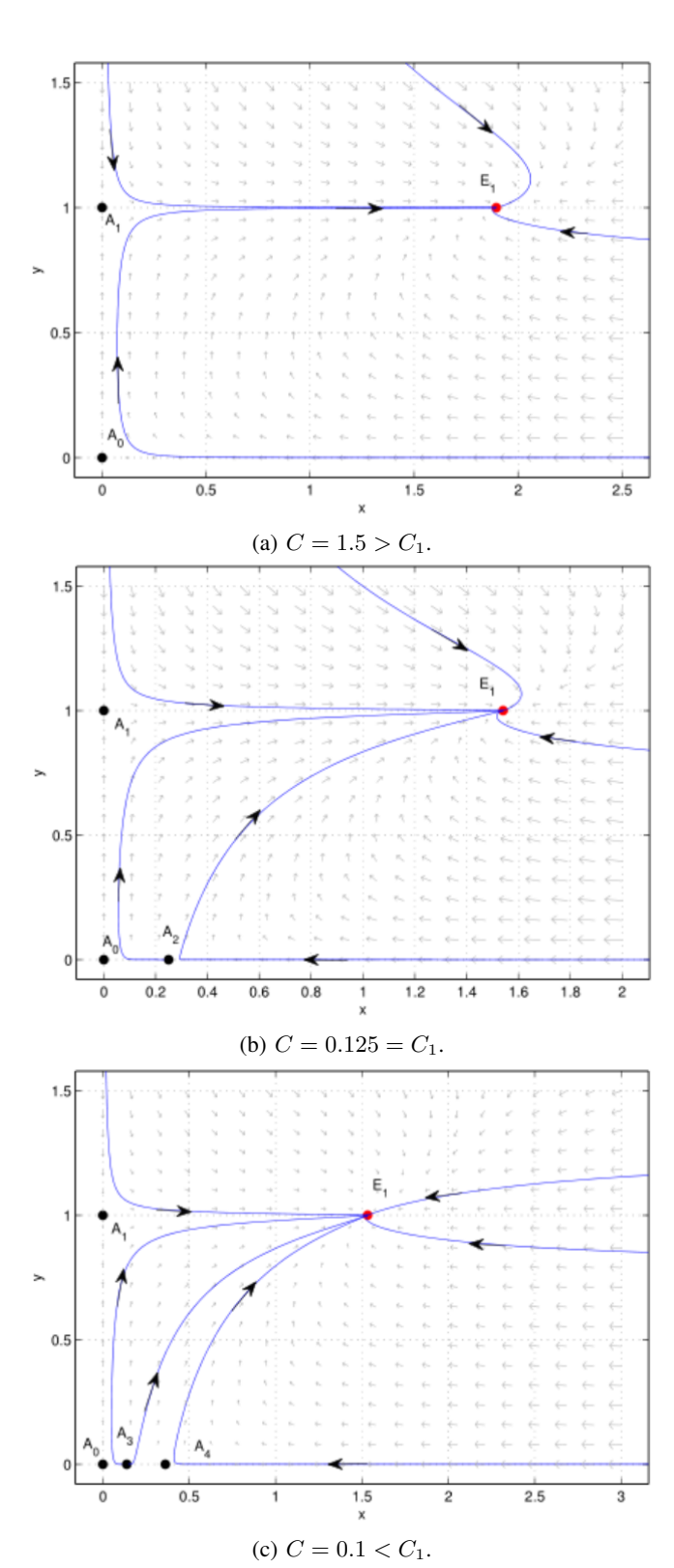


Fig. 4: Case **4** of $r \ge a, r < 1$.

is that the prey abundance at the globally asymptotically stable interior equilibrium is directly influenced by the Allee parameter. Mathematical analysis reveals that the derivative $\frac{\mathrm{d} x_1^*(C)}{\mathrm{d} C} = \frac{a-r}{\sqrt{\Delta_2}} > 0 \ (r < a) \text{ indicates a positive correlation}$ between Allee intensity and equilibrium prey density. This implies that, under controlled harvesting (r < a), an increase in the Allee effect paradoxically leads to higher prey population levels—a counterintuitive result that contrasts sharply

with most ecological models incorporating Allee effects. However, excessive harvesting $(r \geq a+1)$ drives the prey population toward extinction, destabilizing the entire system. This highlights a critical trade-off: while moderate harvesting and Allee effects can sustain or even enhance prey density, overexploitation inevitably leads to collapse. To ensure long-term species coexistence, adaptive management strategies must be implemented. Specifically, establishing harvest-free protected zones can mitigate overexploitation risks, allowing both prey and predator populations to stabilize and thrive under sustainable conditions.

This study underscores the delicate balance between exploitation and conservation in ecological systems subject to Allee effects. The unusual positive relationship between Allee intensity and prey abundance challenges conventional ecological theory and suggests that species responses to Allee thresholds may be more complex than previously assumed.

Remark

This research provides foundational insights into the existence and stability properties of equilibria within a Lotka-Volterra commensalism framework adding both weak Allee effect and linear harvesting in the prey population. In the future, translating these theoretical findings into practical applications represents the critical next step. Key priorities include: (1) Experimentally validating predicted critical resilience points in regulated ecosystems (e.g., mesocosm studies or fisheries with documented harvest histories); (2) Comparative efficacy assessment of extant harvest protocols via historical resource depletion archives.

REFERENCES

- [1] L. L. Xu, Y. L. Xue, Q. F. Lin, F. D. Chen, "Stability and Bifurcation Analysis of Commensal Symbiosis System with the Allee Effect and Single Feedback Control," *International Journal of Applied Mathematics and Computer Science*, vol. 54, no. 8, pp. 1586-1596, 2024.
- [2] D. Ditta, P. A. Naik, R. Ahmed and Z. X. Huang, "Exploring periodic behavior and dynamical analysis in a harvested discretetime commensalism system," *International Journal of Dynamics and Control*, vol. 13, no. 2, Paper No. 63, 12 pp, 2025.
- [3] F. D. Chen, Y. M. Chen, Z. Li, L. J. Chen, "Note on the persistence and stability property of a commensalism model with Michaelis-Menten harvesting and Holling type II commensalistic benefit," *Applied Mathematics Letters*, vol. 134, no. 2, Paper No. 108381, 8 pp, 2022.
- [4] O. Osvaldo, V. P. Geiser, "A seasonal commensalism model with a weak Allee effect to describe climate-mediated shifts," *Selecta Mathematica*, vol. 11, no. 2, pp. 212–221, 2024.
- [5] Y. Wang, "Permanence and stability for a competition and cooperation model of two enterprises with feedback controls on time scales," *IAENG International Journal of Applied Mathematics*, vol. 51, no. 3, pp. 630-636, 2021.
- [6] M. Z. Qu, "Dynamical analysis of a Beddington-DeAngelis commensalism system with two time delays," *Journal of Applied Mathematics and Computing*, vol. 69, no. 6, pp. 4111–4134, 2023.
- [7] X. Q. He, Z. L. Zhu, J. L. Chen, and F. D. Chen, "Dynamical analysis of a Lotka Volterra commensalism model with additive Allee effect," *Open Mathematics*, vol. 20, no. 2, pp. 646–665, 2022.
- [8] F. D. Chen, Q. Zhou, S. Lin, "Global stability of symbiotic model of commensalism and parasitism with harvesting in commensal populations," WSEAS Transactions on Mathematics, vol. 21, no. 1, pp. 424–432, 2022.
- [9] Z. Wei, Y. H. Xia, T. H. Zhang, "Stability and bifurcation analysis of a commensal model with additive Allee effect and nonlinear growth rate," *International Journal of Bifurcation and Chaos*, vol. 31, no. 13, Paper No. 2150204, 17 pp, 2021.
- [10] R. Y. Han, F. D. Chen, "Global stability of a commensal symbiosis model with feedback controls," *Communications in Mathematical Biology and Neuroscience*, vol. 2015, no. 15, 2015.

- [11] W. C. Allee, Animal Aggregations: A Study in General Sociology, University of Chicago Press, USA, 1932.
- [12] F. D. Chen, Z. Li, Q. Pan, Q. Zhu, "Bifurcations in a Leslie–Gower predator–prey model with strong Allee effects and constant prey refuges," *Chaos, Solitons and Fractals*, vol. 192, no. 86, No. 115994, 2025.
- [13] F. D. Chen, Z. Li, Q. Pan, Q. Zhu, "Dynamical analysis of a discrete two-patch model with the Allee effect and nonlinear dispersal," *Mathematical Biosciences and Engineering*, vol. 21, no. 4, pp. 5499–5520, 2024.
- [14] S. M. Chen, F. D. Chen, V. Srivastava, R. D. Parshad, "Dynamical analysis of a Lotka-Volterra competition model with both Allee and fear effects," *International Journal of Biomathematics*, vol. 17, Paper No. 2350077, 48 pp, 2024.
- [15] Q. Zhu, F. D. Chen, "Impact of fear on searching efficiency of first species: a two species Lotka-Volterra competition model with weak Allee effect," *Qualitative Theory of Dynamical Systems*, vol. 23, no. 3, Paper No. 143, 31 pp, 2024.
- [16] X. H. Huang, L. J. Chen, Y. Xia, F. D. Chen, "Dynamical analysis of a predator-prey model with additive Allee effect and migration," *International Journal of Bifurcation and Chaos*, vol. 33, no. 15, Paper No. 2350179, 24 pp, 2023.
- [17] K. Fang, Z. L. Zhu, F. D. Chen, Z. Li, "Qualitative and Bifurcation Analysis in a Leslie-Gower Model with Allee Effect," *Qualitative Theory of Dynamical System*, vol. 21, no. 86, pp. 1-19, 2022.
- [18] K. Fang, J. B. Chen, Z. L. Zhu, F. D. Chen, X. Y. Chen, "Qualitative and Bifurcation Analysis of a Single Species Logistic Model with Allee Effect and Feedback Control," *IAENG International Journal of Applied Mathematics*, vol. 52, no. 2, pp. 320-326, 2022.
- [19] T. T. Liu, L. J. Chen, F. D. Chen, Z. Li, "Stability analysis of a Leslie-Gower model with strong Allee effect on prey and fear effect on predator," *International Journal of Bifurcation and Chaos*, vol. 32, no. 6, pp. 1-24, 2022.
- [20] Z. L. Zhu, M. X. He, Z. Li and F. D. Chen, "Stability and Bifurcation in a Logistic Model with Allee Effect and Feedback Control," International Journal of Bifurcation and Chaos, vol. 30, no. 15, pp. 2050231, 2020.
- [21] Z. W. Xiao, Z. Li, "Stability and Bifurcation in a Stage-structured Predator-prey Model with Allee Effect and Time Delay," *IAENG International Journal of Applied Mathematics*, vol. 49, no. 1, pp. 6-13, 2019
- [22] Y. Y. Lv, L. J. Chen, F. D. Chen and Z. Li, "Stability and Bifurcation in an SI Epidemic Model with Additive Allee Effect and Time Delay," *International Journal of Bifurcation and Chaos*, vol. 31, no. 4, pp. 2150060, 2020.
- [23] Q. F. Lin, "Stability analysis of a single species logistic model with Allee effect and feedback control," *Advances in Difference Equations*, vol. 2018, no. 1, pp. 190, 2018.
- [24] H. Wu, Z. Li, M. X. He, "Bifurcation analysis of a Holling-Tanner model with generalist predator and constant-yield harvesting," *Interna*tional Journal of Bifurcation and Chaos, vol. 34, no. 2450076, 2024.
- [25] C. P. Huang, F. D. Chen, Q. Zhu, Q. Q. Li, "The Dynamic Behaviors of Nonselective Harvesting Lotka-Volterra Predator-Prey System With Partial Closure for Populations and the Fear Effect of the Prey Species," *IAENG International Journal of Applied Mathematics*, vol. 53, no. 3, pp. 818-825, 2023.
- [26] Q. Q. Li, F. D. Chen, L. J. Chen and Z. Li, "Dynamical analysis of a discrete amensalism system with Michaelis-Menten type harvesting for the second species," *Qualitative Theory of Dynamical System*, vol. 23, no. 279, pp. 1-43, 2024.
- [27] Y. C. Xu, Y. Yang, F. W. Meng and S. G. Ruan, "Degenerate codimension-2 cusp of limit cycles in a Holling-Tanner model with harvesting and anti-predator behavior," *Nonlinear Analysis: Real World Applications*, vol. 76, no. 103995, 2024.
- [28] Z. L. Zhu, F. D. Chen, L. Q. Lai, Z. Li, "Dynamic Behaviors of a Discrete May Type Cooperative System Incorporating Michaelis-Menten Type Harvesting," *IAENG International Journal of Applied Mathematics*, vol. 50, no. 3, pp. 458-467, 2020.
- [29] C. C. García, "Bifurcations on a discontinuous Leslie-Grower model with harvesting and alternative food for predators and Holling II functional response" *Communications in Nonlinear Science and Numerical Simulation*, vol. 116, no. 106800, 2023.
- [30] F. D. Chen, "On a nonlinear non-autonomous predator-prey model with diffusion and distributed delay," *Applied Mathematics and Com*putation, vol. 180, no. 1, pp. 33-49, 2005.
- [31] Z. F. Zhang, "Proof of the uniqueness theorem of limit cycles of generalized lienard equation," *Applicable Analysis*, vol. 23, no. 1-2, pp. 63-76, 1986.
- [32] L. S. Chen, *Mathematical models and methods in ecology*, Science Press, Beijing, 1988. (in Chinese).

[33] L. Perko, Differential Equations and Dynamical Systems, Springer, New York, 2013.